

An Image Reconstruction Algorithm for Electrical Capacitance Tomography Based on Simulated Annealing Dual Particle Swarm Collaborative Optimization

^{1,*} Pai Wang, ² J.S. Lin, ¹ M. Wang and ³ Y.L. Zhao

Abstract

Electrical Capacitance Tomography (ECT) image reconstruction is a nonlinear inverse problem with serious ill. Since sensitivity field in the sensor of an electrical capacitance tomography system is "soft field", the "soft field" nature is ignored by the traditional image reconstruction algorithms for ECT. There is the bottleneck in improving the imaging accuracy for the algorithms. To solve the problem, a novel image reconstruction algorithm is developed with simulated annealing dual particle swarm collaborative optimization. In the algorithm, to eliminate the impact generated by the soft field nature of ECT sensitivity field, some image samples with typical flow patterns are chosen for training with LS-SVM. Under the training procedure, the capacitance error caused by the "soft field" nature is predicted, and then is used to construct the fitness function of the particle swarm optimization based on the capacitance error. To avoid falling into local convergence, the dual group cooperative-competition scheme is used. The diversity of particles is increased by intraspecific and intraspecific learning and competition. To speed up the convergence rate, the algorithm introduces simulated annealing ideas into particle swarm optimization, which adopts cooling process functions to replace the inertia weight function and construct the time variant inertia weight function featured in annealing mechanism. Therefore, the algorithm improves the globe convergence and convergence rate. Experimental results demonstrated that the proposed novel algorithm is featured in quick convergence rate and higher imaging precision.

Keywords: Electrical Capacitance Tomography, Lotka-Volterra Model, Simulated Annealing, Least Squares Support Vector Machines, Particle Swarm Optimization.

Paper submitted 08/15/11; revised 11/15/11; accepted 12/30/11.

**Corresponding Author: Pai- Wang*

(E-mail:wangpai2013@xust.edu.cn).

¹*School of Electric and Control of Xi'an University of Science and Technology, Xi'an, China, No. 58, Yanta Road*

²*Department of Computer Science and Information Engineering at National Chin-Yi University of Technology, Taichung, Taiwan*

³*School of Aerospace Science & Technology Xidian University, Xi'an, China, No. 2, Taibai Road*

1. Introduction

As one of the electrical process tomography imaging technologies, Electrical Capacitance Tomography (ECT) is featured in lower costs, no-irradiative and non-invasive methods, etc. and applicable to the visible measurement of two-phase and multiple-phase flows [1-4]. The principle of ECT can be described as: different objects have different permittivities. If the concentration and composition of the component phase is changed, the permittivity will change to fit the mixture. Variation in permittivity will cause the change of the capacitance measurements, and the capacitance measurements reflect the size and distribution of the medium phase concentration of the mixture. On this basis, a corresponding image reconstruction algorithm can be used to reconstruct the distribution of the test area of the pipeline.

Because ECT is non-linearity, and the number of capacitances independently measured are much less than the number of pixels for image reconstruction, there is no resolution for the reverse problem. Furthermore, the sensitivity field of ECT is featured in "soft field", i.e. sensitivity not evenly distributed, and the reverse problem equation is in a seriously abnormal state [5]. Therefore, an image reconstruction algorithm has been the bottleneck for the further development of ECT, and a highly precise image reconstruction algorithm is required.

The existing ECT image reconstruction algorithms can be divided into two main types: non-iterative algorithm and iterative algorithm. As one of the typical non-iterative algorithms, Linear Back Projection (LBP) is simple and quick, but unsatisfying in imaging precision. Therefore, LBP is only used as a qualification method [6]. Iterative methods include: Tikhonov regularization method, Landweber algorithm, Newton-Raphson algorithm etc [7]. Tikhonov method may cause detailed distortion of the reconstructed images due to over-smoothness of regularization functions. As a widely used method in recent years, Landweber returns satisfying results only with large number of iterations as to complex flow patterns. Newton-Raphson algorithm is featured in local convergence, but the iterative convergence can't be guaranteed if the initial value is selected appropriately or not.

In this paper, we introduce an image reconstruction algorithm with least squares support vector machine (LS-SVM) and Lotka-Volterra Annealing Dual Particle Swarm Collaborative Optimization (LV-ADPSO). The proposed novel algorithm is described as follows: firstly, we construct LS-SVM and excise the error between the capacitances arising from sensitivity matrix and the actual capacitance measurements; then based on the error, we constructed the fitness function and simulated annealing mechanism for the dual particle swarm collaborative optimization; finally, we search for the optimum solution for image reconstruction with LV-ADPSO.

2. Electrical Capacitance Tomography System

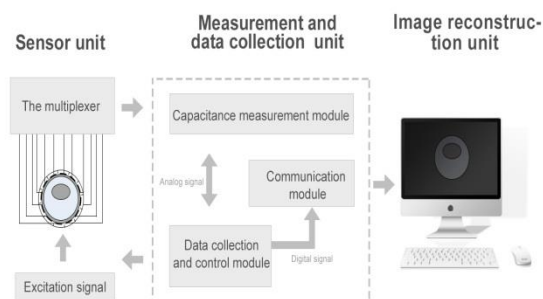


Figure 1: Constitutes of ECT system.

As shown in Figure 1, ECT System is mainly consisted with three units: a capacitance sensor unit, a measurement and data collection unit, and an image reconstruction unit. By utilizing capacitive fringe effect, the sensor can produce a corresponding capacitance for a medium with certain permittivity. The combination of all sensing electrodes may provide multiple capacitance measurements, which can be taken as the projection data for image reconstruction. The capacitance measurement and data collection unit primarily function as rapidly, stably and accurately measuring minor capacitance. It changes in various arrays of electrode couples, and transmits the acquired data to a computer. This unit is mainly comprised of three modules: a capacitance measurement module, a data collection control module, and a communication module. The capacitance measurement module is used to realize the switching of CV (capacitance to voltage) to measure minor capacitance and effectively inhibit stray capacitance [8]. The data collection control module generally takes DSP as the control core and takes ADC for data acquisition. Data communication adopts USB2.0 Technology [9]. ECT image reconstruction unit is composed of two parts:

hardware and software. Hardware indicates a general-purpose computer, and software indicates image reconstruction algorithm.

ECT image reconstruction process includes forward and reverse questions to be resolved. As the forward question, capacitance values of all electrode pairs based on the permittivity distribution and excitation voltages of the known sensitivity field. The mathematic model of forward question of ECT is expressed as follows [7]:

$$C_{i,j} = \iint_D \varepsilon(x,y) \cdot S_{i,j}(x,y) dx dy \quad (1)$$

where $C_{i,j}$ is the capacitance between the electrode pair of $i-j$, $\varepsilon(x,y)$ is the permittivity distribution on cross-section of pipes, $S_{i,j}(x,y)$ is the sensitivity functions when the capacitance between electrode pair of $i-j$ is distributed on the cross-section of pipe, and D is the electrode surface. It can be seen that the sensitivity of the electrode in a point is related to its position, namely the sensitivity is not evenly distributed within the sensitivity field, which is the so-called effects of "soft field". If the "soft field" nature is ignored, Equation (1) shall be linearized and discredited to get

$$C = S \cdot G \quad (2)$$

where C is a normalization capacitance vector of m dimension, G is n dimension normalized permittivity distribution vector, i.e. the grey level of pixels for visualization, and S is $m \times n$ factor matrix, which reflects influence of medium distribution variation on capacitance C and is called as sensitivity matrix [10]. Note that, the matrix S is not truly constant, but varies with the actual permittivity distribution. Therefore, most of the image reconstruction algorithms are achieved based on Equation (2) which is bound to have a greater approximation error.

3. An Algorithm Design for ECT Image Reconstruction

3.1 Particle Swarm Optimization Algorithm

Particle swarm optimization (PSO) is a well known heuristic algorithm, which was first proposed by Kennedy and Eberhart in 1995 and was sourced from studies on food-catching of birds [11-13]. In PSO system, each alternative resolution is called as a "particle". Particles are co-exist and shall be optimized. That is because each particle should "fly" towards to a better position in the question space according to its own experiences to explore the best resolution. The mathematic expression of PSO is shown as follows [14].

We presume that the space is D -dimension and total numbers of particles are N . Position of i th particle expressed as $X_i = (x_{i1}, x_{i2}, \dots, x_{iD})$; The best position of the i th particle in "flying" history is $P_i = (p_{i1}, p_{i2}, \dots, p_{iD})$, presume the best value of $P_i (i = 1, 2, \dots, N)$ is located at P_g ; the variance rate of the i th particle is the vector of $V_i = (v_{i1}, v_{i2}, \dots, v_{iD})$; position of each particle shall change according to the following equations:

$$v_{id}(t+1) = \omega \cdot v_{id}(t) + c_1 \cdot r_1 \cdot [P_{id}(t) - x_{id}(t)] + c_2 \cdot r_2 \cdot [P_{gd}(t) - x_{id}(t)] \quad (3)$$

$$x_{id}(t+1) = x_{id}(t) + v_{id}(t+1) \quad (4)$$

Where, c_1 and c_2 are positive constant and called as speedup factor; r_1 and r_2 are the random number between $[0,1]$; ω is called as inertia factor; i is the i th particle $1 \leq i \leq N$, and d is d th dimension of each particle $1 \leq d \leq D$. The initial position and speed of particle swarm is generated at random, and then iterated according to Equations (3) and (4). The position variance range and speed variance range is separately $[-x_{d,\max}, x_{d,\max}]$ and $[-v_{d,\max}, v_{d,\max}]$. The boundary value shall be taken if x_{id} or v_{id} of one dimension exceeds the boundary.

3.2 Simulated Annealing Dual Particle Swarm Collaborative Optimization

Only using the standard PSO algorithm for image reconstruction is difficult to find the optimal solution. If using standard particle swarm optimization algorithm to solve the high dimensional problems, the results often fall into local convergence. In order to get high resolution reconstructed image, the particles (i.e. permittivity distribution vector) G_K must have a high dimension.

Many studies have shown that the cause of local convergence is the loss of particle diversity [15-18]. In order to keep the diversity of particles, the novel algorithm introduces Lotka-Volterra model into PSO, and designs the dual particle swarm cooperative-competition scheme. Collaborative optimization of particle are affected by three major factors in the optimization process:[19] 1 Individual fitness of particles, 2 Living environment of particle, 3 Competition among the particles. It takes full account of the various relationships between groups, and greatly increases the diversity of the particles.

We presume the scale of A group is N_A , and the scale of B group is N_B . The position and velocity of i th particle which in the A group will change according to the following equations:

$$v_i^A(t+1) = \omega \cdot v_i^A(t) + c_1^A \cdot r_{1i}^A \cdot [P_i^A(t) - x_i^A(t)] + c_2^A \cdot r_{2i}^A \cdot [P_g^A(t) - x_i^A(t)] + c_3^A \cdot r_{3i}^A \cdot [P_g(t) - P_g^B(t) - 2x_i^A(t)] \quad (5)$$

$$(t+1) = x_i^A(t) + v_i^A(t+1) \quad (6)$$

Where i is the i th particle $1 \leq i \leq N_A$. $v_i^A(t)$ is the velocity of the i th particle in the A group. $x_i^A(t)$ is the position of the i th particle in the A group. $c_1^A = 2.15$, $c_2^A = 1.03$. r_{1i}^A , r_{2i}^A and r_{3i}^A are random numbers between $[0,1]$. $P_i^A(t)$ is the best position of the i th particle in the "flying" history. $P_g^A(t)$ is the best of $P_i^A(t)$.

The position and velocity of j th particle in the B group will change according to the following equations

$$v_j^B(t+1) = \omega \cdot v_j^B(t) + c_1^B \cdot r_{1j}^B \cdot [P_j^B(t) - x_j^B(t)] + c_2^B \cdot r_{2j}^B \cdot [P_g^B(t) - x_j^B(t)] + c_3^B \cdot r_{3j}^B \cdot [P_g(t) - P_g^A(t) - 2x_j^B(t)] \quad (7)$$

$$x_j^B(t+1) = x_j^B(t) + v_j^B(t+1) \quad (8)$$

Where j is the i th particle $1 \leq i \leq N_B$. $v_i^B(t)$ is the velocity of the j th particle which in the B group. $x_i^B(t)$ is the position of the j th particle in the B group. $c_1^B = 2.15$, $c_2^B = 1.03$. r_{1j}^B , r_{2j}^B and r_{3j}^B are random numbers between $[0,1]$. $P_j^B(t)$ is the best position of the j th particle in the "flying" history. $P_g^B(t)$ is the best of $P_j^B(t)$. $P_g(t)$ is the best of the A group and B group, (i.e. image reconstruction of the current optimal solution) and it is according to the following equation[19]:

$$P_g(t) = \min(P_g^A(t), P_g^B(t)) \quad (9)$$

In particle swarm optimization process, each particle of two sub-groups are attracted not only by the globe best in own group and by the different globe best in another group. Thus, the diversity of particles is greatly increased. However, blindly increasing the diversity of the particles will lead to lower convergence rate. Simulated Annealing algorithm is another widely used iterative heuristic algorithm. The powerful feature is its intrinsic hill climbing capability [20-24]. In order to speed up the dual particle swarm collaborative optimization convergence speed, we introduce simulated annealing ideas into dual particle swarm collaborative

optimization which adopts cooling process functions to replace the inertia weight function and construct the time variant inertia weight function featured in an annealing mechanism. The cooling process function is as follow [25]:

$$T(t) = \frac{1}{\tau + 1} [\tau + \tanh(\Omega)'] T(t-1) \quad (10)$$

Where Ω is a constant near to 1, and τ is a constant while t means numbers of iteration. Shown as in Equation (8), we replace ω in Equation (5) and Equation (7) with Equation (10) to construct timing inertia factor reducing with passage of time.

$$\begin{aligned} v_j^B(t+1) = & T(t) \cdot v_j^B(t) + c_1^B \cdot r_{1j}^B \cdot [P_j^B(t) - x_j^B(t)] + \\ & c_2^B \cdot r_{2j}^B \cdot [P_g^B(t) - x_j^B(t)] + \\ & c_3^B \cdot r_{3j}^B \cdot [P_g(t) - P_g^A(t) - 2x_i^B(t)] \end{aligned} \quad (11)$$

$$\begin{aligned} v_j^B(t+1) = & T(t) \cdot v_j^B(t) + c_1^B \cdot r_{1j}^B \cdot [P_j^B(t) - x_j^B(t)] + \\ & c_2^B \cdot r_{2j}^B \cdot [P_g^B(t) - x_j^B(t)] + \\ & c_3^B \cdot r_{3j}^B \cdot [P_g(t) - P_g^A(t) - 2x_i^B(t)] \end{aligned} \quad (12)$$

3.3 Selection of Fitness Functions

In order to overcome the “soft field” nature of ECT sensitivity field, some image samples with typical flow patterns are chosen for training with Least squares support vector machine (LS-SVM) [26-30]. Under the training procedure, the capacitance error caused by the “soft field” nature is predicted, and then is used to construct the fitness function of the particle swarm optimization based on the capacitance error. The fitness function is given as the following:

$$F = \min(\|C - S \cdot G_k\| - \|\Delta C\|) \quad (13)$$

Where $\|\Delta C\|$ is the output when LS-SVM takes C as input. The fitness function uses the results predicted by LS-SVM so as to eliminate errors arising from different flow patterns under the fix sensitivity matrix S .

3.4 Least Squares Support Vector Machine and Its Applications In Image Reconstruction

As the "soft field" effect, for different flow patterns, the priori conditions of $\|\Delta C\|$ are different. Thus some image samples with typical flow patterns are chosen for training with LS-SVM. Under the training procedure, the capacitance error $\|\Delta C\|$ caused by the “soft field” nature is predicted.

Set number of sample images is n , the number of mesh cells of sensitive field is N , and then sample collection of LS-SVM is $\{\bar{G}_i, \Delta C_i\}_{i=1}^n$. Where \bar{G}_i is the N -dimensional normalized vector, $\Delta C_i \in R$. The function estimate expression of the least square algorithm is as follows:

$$\|\Delta C(\bar{G})\| = \sum_{i=1}^n \alpha_i K(x, x_i) + b \quad (14)$$

Where \bar{G} is the permittivity distribution vector to be predicted. $\alpha_i (i=1, 2, \dots, n)$ is the support vector. b is the regression parameter. $K(x, x_i)$ is the kernel function. There are many kinds of kernel functions. In this paper, we take the kernel function of radial basis (i.e. Gaussian) with higher regression capabilities which is defined as follows:

$$K(x, x_i) = \exp\left(-\frac{\|x - x_i\|^2}{\sigma^2}\right) \quad (15)$$

Where, σ means Gaussian kernel parameter

3.5 Algorithmic Process

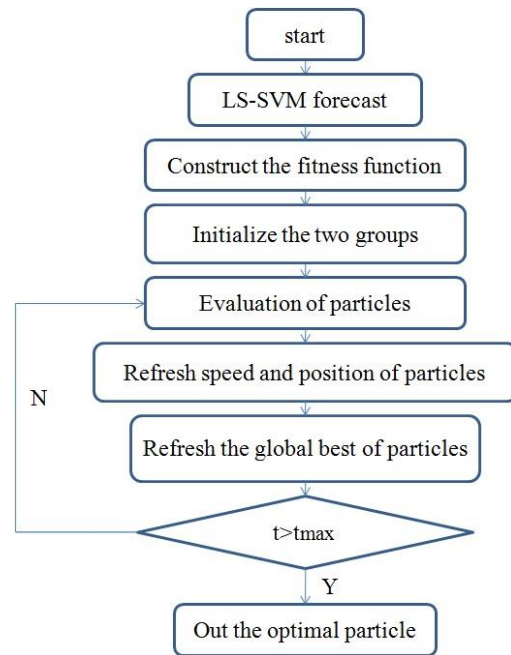


Figure 2: The algorithm flow process.

The algorithm flow process is shown as Figure 2, where t is current iteration times.

- Step 1: LS-SVM exercise forecast stage, the capacitance error caused by the “soft field” nature is predicted.
- Step 2: Construct the fitness function according to Equation (13).
- Step 3: Initialize the two groups, set up parameters of two groups and initialize the position and velocity of each particle.
- Step 4: Evaluate particles and calculate the fitness function of each particle of two groups.
- Step 5: Refresh speed of particles of A group according to Equation (11) and refresh position of particles of A group according to Equation (6). Refresh speed of particles of B group according to Equation (12) and refresh position of particles of B group according to Equation (8).
- Step 6: Refresh the global best of particles of two groups according to Equation (9).
- Step 7: Check the termination condition, if the maximum number of iterations is met, complete the iteration and give the optimum position of particle (i.e. optimum solution); otherwise, go to step 4.

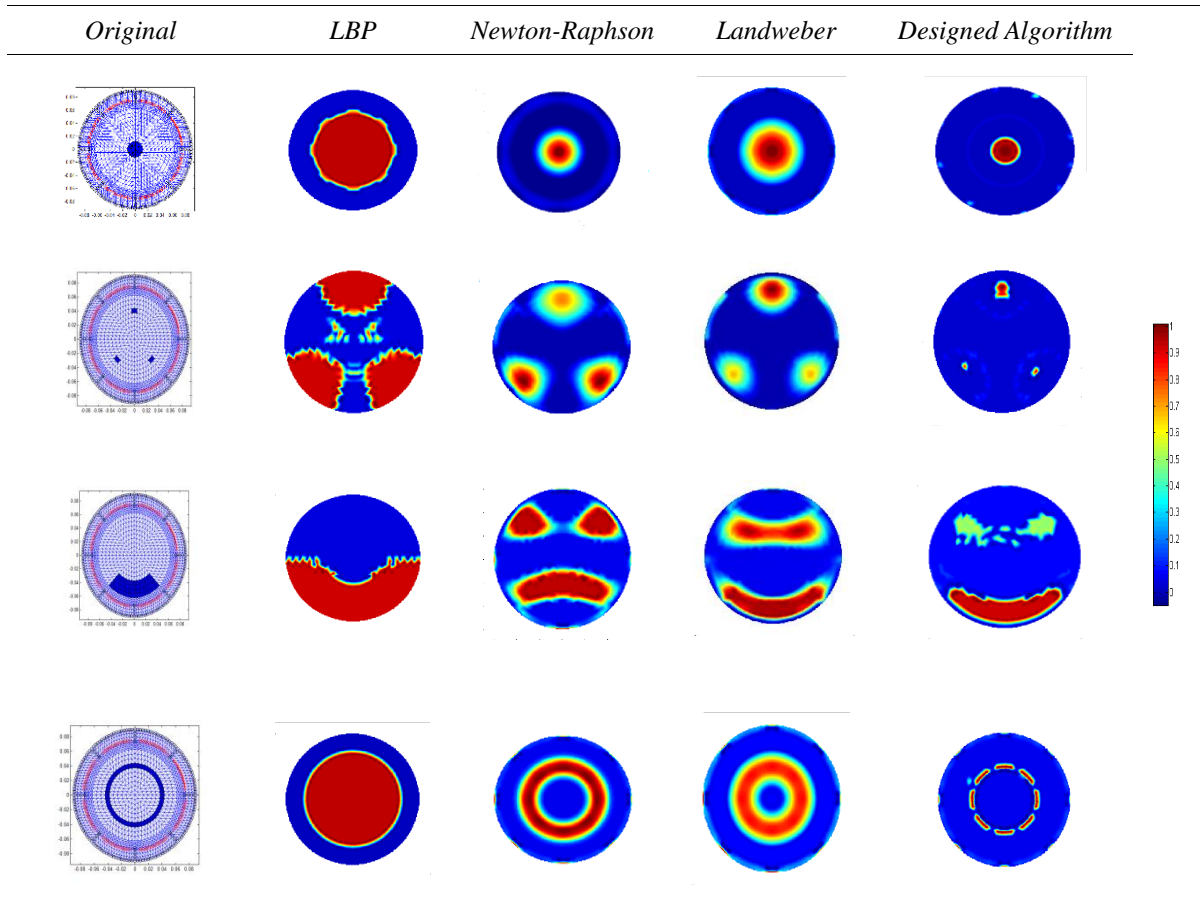
4. Experiment and Analysis

We select 8 electrode capacitance sensors to get 28 separated capacitance measurements, and thus the input sample data of LS-SVM x_i is 28-dimension. Capacitance measurements can be obtained with finite element methods. In finite mesh, we take triangle unit to mesh the imaging area into 800 units, and we take finite subdivision unit as the pixel unit of images, and the permittivity distribution \bar{G} under all kinds of flow patterns of sample is an 800-dimension vector.

In order to validate effectiveness of the algorithm, we designed algorithm to make image reconstruction for typical flow patterns (i.e. core flow, bubble flow, laminar flow and circular flow), and then compared them with the imaging results of LBP algorithm, Newton-Raphson algorithm and Landweber algorithm. The experimental results are shown in Table 1. In the imaging area, the dark area is even medium of permittivity 40, and the other areas is air (i.e. permittivity 1.0).

As shown in Table 1, we can see that position errors are much significant for LBP imaging results compared with the original. Imaging results with Landweber algorithm and Newton-Raphson algorithm are near to the original, but there are too many false images. Obviously, the quality of images obtained with designed algorithm is much better, because the resolution of images is much higher, and there is nearly no false image.

Table 1: Imaging results



When the quality of image is analyzed, the relative image error shall be used as an evaluation index of image quality, which is defined as follows:

$$\mathcal{E}_{image} = \frac{\|\bar{G} - G\|}{\|G\|} \quad (16)$$

Where \bar{G} is a permittivity distribution vector obtained with a reconstruction algorithm, and G is permittivity distribution vector in the original. $\|\cdot\|$ is a vector sample norm, which is taken as 2.

Table 2: Image relative image error

Original	LBP	Newton-Raphson	Landweber	Designed Algorithm
1	85.3%	33%	41.8%	17.3%
2	87.6%	37.6%	40.2%	20%
3	45%	71%	65%	41%
4	87%	32.8%	40.1%	27%

The experimental results of the relative image error are shown in Table 2, From Table 2 we can see that the quality of reconstruction image with the designed algorithm for all above flow types is significantly improved by comparing with LBP Newton-Raphson and Landweber algorithms.

Table 3: Elapsed time

Original	LBP	Newton-Raphson	Landweber	Designed Algorithm
1	0.04s	10.77s 500 iterations	3.61s 100 iterations	5.3s 60 iterations
2	0.04s	11.12s 500 iterations	4.98s 130 iterations	9.10s 120 iterations
3	0.04s	14.05s 800 iterations	7.28s 200 iterations	10.55s 130 iterations
4	0.04s	12.18 600 iterations	33.7s 5000 iterations	12.10s 140 iterations

The elapsed time required for reconstruction of the four different algorithms is shown in table 3. Obviously, LBP is the most fast because it is a non-iterative algorithm. The number of iterations for Landweber and Newton-Raphson algorithms are greater than that for the designed algorithm. This shows that the designed algorithm convergence is faster than that for Landweber and Newton-Raphson algorithms.

5. Conclusions

In this paper, we have introduced an ECT image reconstruction algorithm based on LS-SVM and LA-ADPSO. This algorithm can be divided into two stages: LS-SVM exercise forecast stage and LA-ADPSO search stage. In LS-SVM exercise forecast stage, in order to overcome the soft field nature of ECT sensitivity field, we took LS-SVM to exercise for the errors and apply exercise results to construct the fitness function of the particle swarm optimization. In LA-ADPSO search stage, we introduced Lotka-Volterra model into PSO, so the diversity of particles is great increased. We adopted cooling process functions to replace the inertia weight function and constructed the time variant inertia weight function featured in annealing mechanism. Meanwhile, it employs the LA-ADPSO procedure to search for the optimized resolution of Electrical Capacitance Tomography (ECT) for image reconstruction. The experimental results show that this algorithm is featured in quick convergence rate and higher imaging precision.

Acknowledgment

This work is financially supported by Projects 51405381 and 51475013 from the National Natural Science Foundation of China, Project 201314 supported by Engagement Foundation of Xi'an University of Science and Technology, and a Project supported by Scientific Research Foundation for Returned Scholars, Ministry of Education of China 2011508

References

- [1]. T. York, "Status of electrical tomography in industrial applications," *Electronic Imaging*, vol. 10, no. 3, pp. 600-619, 2001.
- [2]. C. Tan, F. Dong and M. Wu, "Identification of gas/liquid two-phase flow regime through ERT-based measurement and feature extraction," *Flow Meas. Instrum.*, vol.18, no.5, pp. 255-261, 2007.
- [3]. W. Yin and A. J. Peyton, "A planar EMT system for the detection of faults on thin metallic plates," *Meas. Sci. Technol.* vol.17, pp. 2130-2135, 2006.
- [4]. H. Griffiths, "A phantom for electrical impedance tomography", *Clin. Phys. Physiol. Meas.* 9: Suppl. A, pp.15-20, 1988.
- [5]. W. Q. Yang, "Modeling of capacitance tomography sensors", *IEE Proceedings: Science, Measurement and Technology*, vol. 114 no. 3, pp: 203-208, 1997.
- [6]. L. H. Peng, D. Lu, and W.Q. Yang, "Image reconstruction algorithms for electrical capacitance tomography: state of the art", *Tsinghua Univ. (Sci. & Tech.)*, vol. 44 no.4, pp: 478-484, 2004.
- [7]. L. H. Peng, P. Jiang, G. Lu, and D. Xiao, "Window function-based regularization for electrical capacitance tomography image reconstruction", *Flow Meas. Instrum.*, vol. 18 no.5-6, pp. 277-284, 2007.
- [8]. W. Q. Yang, "Hardware design of electrical capacitance tomography systems," *Meas. Sci. Technol.* vol. 7, pp. 225-232, 1996.
- [9]. D.Y. Yang, C.L. Xu, and B. Zhou, "Electrical capacitance tomography system based on single measurement channel", *Chinese Journal of Scientific Instrument*, vol.31, no.1, pp: 132-136, 2010.
- [10]. A.N. Tikhonov, and V.Y. Arsenin, *Solutions of ill-posed problems*, Washington, DC: Winston, First edition, 1977.
- [11]. R. Eberhart, and J. Kennedy, "A New Optimizer Using Particles Swarm Theory", In *Proceedings of the Sixth International Symposium on Micro Machine and Human Science*, 1995.
- [12]. H. Rezazadeh, M. Ghazanfri, and S.J. Sadjadi, "Linear programming embedded particle swarm optimization for solving an extended model of dynamic virtual cellular manufacturing systems", *Journal of Applied Research and Technology*, vol.7 no. 1, pp:83-108, 2009.
- [13]. K. E. Parspulos, and M. N. Vrahatis, "Recent Approaches to Global Optimization Problems Through particle swarm optimization," *Nature Computing*, vol. 1, no. 2-3, pp. 325-306, 2002.
- [14]. R Eberhart, and Y. Shi, "Comparing inertia weights and constriction factors in Particle Swarm Optimization", In *Proceedings of the Congress on Evolutionary Computation 2000*.
- [15]. T. Blackwell, and J. Brank, "Multiswarms exculsion and anticonvergence in dynamic environment", *IEEE Tans on Evolutionary Computation.*, vol.10 no. 4, pp.459-472, 2006.

- [16]. A. Gerardo, O.C. Mauricio, C.C. Nareli, B.F. Ricardo, and A.A.C. Jessus, "Comparative Study of Parallel Variants for a Particle Swarm Optimization Algorithm Implemented on a Multithreading GPU", *Journal of Applied Research and Technology*, vol.7 no. 3, pp. 292-309, 2009.
- [17]. B. Alatas, E. Akin, and A.B. Ozer, "Chaos embedded particle swarm Optimization algorithms," *Chaos Solutions& Fractals*. vol.40, no.4, pp. 1715-1734, 2009.
- [18]. Krilc, T., Vesterstrom, J.S., and Riget, J., "Particle swarm optimization with spatial particle extension". *Proceedings of the World on Congress on Computational Intelligence*. 1474-1479, 2002.
- [19]. X.X. Wu B.L. Guo and J. Wang, "Lotka-Volterra model based particle swarm optimization", *Control and Decision*, vol.25, no. 11, pp.1619-1624, 2010.
- [20]. S. Kirkpatrick, "Optimization by simulated annealing", *Science*, vol.220, pp:671-680, 1983.
- [21]. C. Chen, C.X. Zhao, "Path test data generation based on chaos anneal particle swarm optimization", *Journal of Nanjing University of Science and Technology*. vol.3, pp.376-381. 2009.
- [22]. J. Lv, B.Q. Qin, and B. Li, "Two-Phase Genetic- annealing Algorithm for Vehicle Routing Problem with Mutiple Constraints," *Journal of Xi'an Jiao Tong University*, vol. 39, no.12,pp. 1329-1302,. 2005.
- [23]. M. Marchesi, G. Molinari, M. Repetto, "A parallel simulated annealing algorithm for the design of magnetic structures," *IEEE Transactions on Magnetics* , vol.5, pp.3439-3442, 1994.
- [24]. S. J. Redmond, E. Heneghanc " A method for initialising the K-means clustering algorithm using kd-trees," *Pattern Recognition Letters*, vol. 08, pp.965-973, 2007.
- [25]. J. S Lin, "Annealed chaotic neural network with nonlinear self-feedbackand its application to clustering problem", *Pattern Recognition*, vol.34, no. 5, pp. 1093-1104, 2001.
- [26]. Y. P. Gu, W. J. Zhao, and Z. S. Wu, "Least squares vector machine algorithm". *Journal of Tsinghua University (Science & Technology)*. vol 50, pp.1063-1066, 2010.
- [27]. V N. Vapnik, "The Nature of Statistical Learning Theory", New York:Springer-Verlag, 1995.
- [28]. C. Cortes, V. Vapnik, "Support vector networks" *Machine Learning*, vol.12, no. 5, pp.273-297. 1995.
- [29]. Y. C. Tang, B. Jin, and Y. Q. Zhang, "Granular support vector machines with association rules mining for protein homology prediction".*Artificial Intelligence in Medicine*,vol. 1, pp.121-134, 2005.
- [30]. S. F. Ding, B. J. Qi, " Research of granular support vector machine", *Artificial Intelligence Review*, 2012, vol. 1, pp.1-7, 2012.



Pai, Wang was born in Dandong, Liao Ning Province, China, in 1979. He received his B.S. degree in Computer technology and Application from Xidian University, Xi'an, China, in 2003 and the M.S. degree in Measurement

Technology & Instruments, from Xidian University, in 2008. Hereceived Ph.D. degree in Measurement technology& Instruments, from Xidian University, in 2013. Since 2013 he has been a Lecturer with School of Electric and Control of Xi'an University of Science and Technology. His research interest includes Non-destructive testing technology, Electrical Resistance Tomography, The inverse problem in image processing.



Jzau-Sheng, Lin was born in Taiwan, in 1956, He received the B.S. degree in Electronic Engineering from Taiwan University of Science and Technology in 1980, the M.S. and Ph.D. degrees in Electrical Engineering from National

Cheng Kung University in 1989 and 1996 respectively. He is a Professor of the Department of Electronic Engineering at National Chin-Yi Institute of Technology, Taichung, Taiwan, ROC. His research interests involve neural network, image compression, pattern recognition, and medical image analysis, and EEG.



Mei, Wang was born in Anhui province, China, in 1965. She received the B.S. degrees in Automation in 1985 from Changsha Railway Institute, and the M.S. degree in Automation in 1990, and the Ph.D. degrees in Safety Technology and Engineering in 2006 from Xian University of Science and Technology. Since 2004, she has been a Professor in College of Electric and Control Engineering in Xi'an University of Science and Technology. From July 2007 to July 2008, she studied as a visiting professor in Imperial College London, U.K. From 2012 to 2013, she was a visiting professor in National Chin-Yi University of Technology, Taiwan. Her research interests include control system and pattern recognition.



Yu-Lei, Zhao was born in 1983. He received his B.S. degree in Measurement technology & Instruments from Xidian University, Xi'an, China, in 2008 and the M.S. degree in Measurement technology & Instruments, from Xidian University, in 2010. PhD candidate His research interest includes Non-destructive testing technology, Electrical Capacitance Tomography, image processing.